PHILOSOPHICAL TRANSACTIONS OF THE ROYAL SOCIETY A MATHEMATICAL, PHYSICAL & ENGINEERING SCIENCES

Influence of reactive solute transport on spreading kinetics of alloy droplets on ceramic surfaces

The Royal Society

Phil. Trans. R. Soc. Lond. A 1998 **356**, 871-884
doi: 10.1098/rsta.1998.0193

The Royal Society

Influence of reactive solute transport on spreading kinetics of alloy droplets on ceramic surfaces

By N. Eustathopoulos[1], J. P. Garandet[2] and B. Drevet[2]

[1]*Laboratoire de Thermodynamique et Physico-Chimie Métallurgiques, UMR 5614 CNRS-INPG-UJF, Ecole Nationale Supérieure d'Electrochimie et d'Electrométallurgie de Grenoble, Institut National Polytechnique de Grenoble, BP 75 Domaine Universitaire, 38402 Saint-Martin d'Hères Cedex, France*

[2]*Commissariat à l'Energie Atomique, DTA/CEREM/DEM/SPCM, Laboratoire de Recherche de Base en Solidification, 17 rue des Martyrs, 38054 Grenoble Cedex 9, France*

This paper focuses on the question of the processes which can be rate-limiting for reactive spreading in the sessile drop configuration. It will be shown that for a class of systems, spreading kinetics is controlled by the transport of species involved in the reaction between the drop bulk and the triple line. For these systems convection, and especially Marangoni convection, may significantly affect the dynamics of wetting.

Keywords: wetting; reactivity; interfaces; diffusion; Marangoni convection

1. Introduction

In non-reactive metal–ceramic systems non-wetting is usually observed, the angle θ formed at the contact line of three phases, solid (S), liquid (L) and vapour (V), being greater than 90° (Naidich 1981; Eustathopoulos & Drevet 1994). Typical examples are the couples Cu–Al_2O_3 and Cu–C_{gr}, for which the contact angle under high vacuum or in inert gas is as large as 130–140° (Naidich 1981). However, in several fields of materials science, e.g. joining of ceramics by brazing alloys or metal–ceramic multimaterial processing by infiltration routes, good wetting is required (θ much lower than 90°). Although some improvement in wetting and adhesion may be produced by tensioactive solutes (Eustathopoulos & Drevet 1994), acting by adsorption at the metal–ceramic interface, strong effects on these properties can be obtained by specific reactive solutes forming, by reaction with the ceramic at the interface, continuous layers of a new compound (Nicholas 1986; Loehman & Tomsia 1988; Nogi 1993). Due to uncertainties on the driving force of reactive wetting and to the complexity of kinetic phenomena in the sessile drop configuration, no fundamental approach has been developed until recently on spreading kinetics in reactive systems.

This paper reviews the main results obtained on the dynamics of wetting in reactive systems during the period 1993–96. In § 2 the question of reactive wetting driving force is discussed. In § 3, the different processes which may be rate-limiting are considered, namely viscous flow, local chemical kinetics and solute diffusion. A new analysis of the possible effect on wetting kinetics of convection in the liquid drop is also presented. All experimental results given below were obtained by the sessile

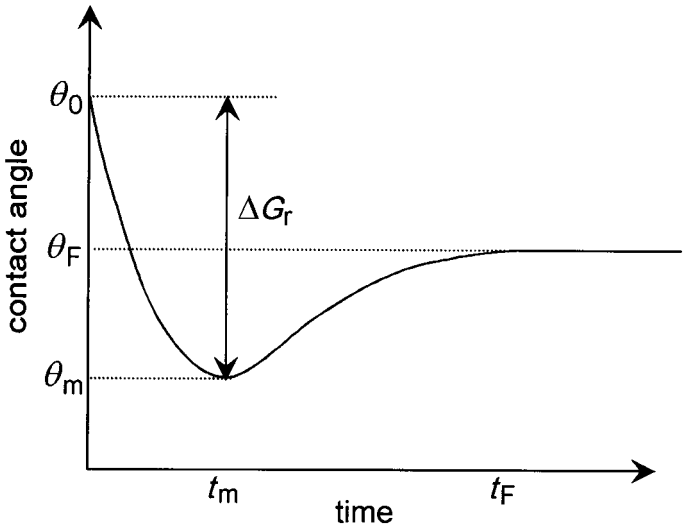

Figure 1. Contact angle versus time curve in a reactive system according to the model of Aksay *et al.* (1974).

drop technique under high vacuum or in inert gas, using millimetre-size droplets and smooth (average roughness of a few nm) monocrystalline (α-Al_2O_3, SiC) or vitreous (carbon) substrates. Although different kinds of reaction can affect wetting (for instance the simple dissolution of an oxide in the liquid alloy (Eustathopoulos & Drevet 1994)) the paper focuses on interfacial reactions leading to the formation of a dense layer of solid reaction product.

2. Driving force of reactive wetting

When a pure liquid wets the smooth and chemically homogeneous surface of an inert solid, the wetting driving force at time t is given by

$$F_{\mathrm{d}}(t) = \sigma^0_{\mathrm{SV}} - \sigma^0_{\mathrm{SL}} - \sigma^0_{\mathrm{LV}} \cos\theta(t), \tag{2.1}$$

where σ^0_{ij} are the characteristic surface energies of the system, and $\theta(t)$ is the instantaneous contact angle. At equilibrium, $F_{\mathrm{d}} = 0$, which leads to the classical Young's equation as follows:

$$\cos\theta^0 = \frac{\sigma^0_{\mathrm{SV}} - \sigma^0_{\mathrm{SL}}}{\sigma^0_{\mathrm{LV}}}. \tag{2.2}$$

For reactive solid–liquid systems, no clear definition of the driving force exists at the present time. Aksay *et al.* (1974) replaced the σ^0_{SL} term in equation (2.1) by

$$\sigma_{\mathrm{SL}}(t) = \sigma^0_{\mathrm{SL}} + \Delta G_{\mathrm{r}}(t), \tag{2.3}$$

where $\Delta G_{\mathrm{r}}(t)$ is the change in Gibbs energy released per unit area by the reaction in the 'immediate vicinity of the solid–liquid interface' (Aksay *et al.* 1974).

Aksay *et al.* (1974) argue that the effect of the $\Delta G_{\mathrm{r}}(t)$ term is strongest during the early stages of contact because the interfacial rate is at its maximum when the liquid contacts a fresh unreacted solid surface. Thereafter, the reaction kinetics slow down, and after an initial decrease, the contact angle increases and gradually approaches the equilibrium value (figure 1).

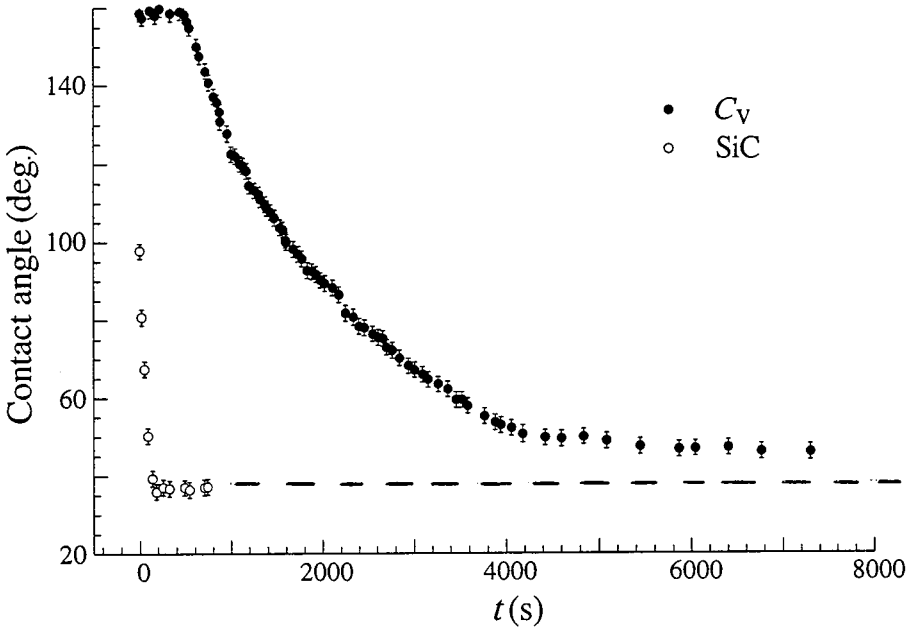

Figure 2. Contact angle kinetics obtained for a Cu-40 at.% Si alloy on vitreous carbon and α-silicon carbide substrates under high vacuum at 1423 K (Landry *et al.* 1997).

A critical discussion of this model, as well as of experiments used to validate it, is given elsewhere (Eustathopoulos 1996). In the present paper, we will describe two recent experiments which disagree with Aksay's model and allow us to propose another interpretation of reactive driving force. The first experiment is a Cu–Si alloy on vitreous carbon (figure 2) (Landry *et al.* 1997). Pure copper does not wet vitreous carbon (at 1150 °C, $\theta = 137 \pm 5°$) but a Cu–40 at.% Si alloy wets well this substrate due to the formation, at the interface, of a continuous submicron layer of SiC. When the experiment is repeated with the same alloy on an α-SiC monocrystalline substrate wetting kinetics are very different: very fast in the non-reactive system (i.e. Cu–Si/SiC) and very slow in the reactive one (Cu–Si/Cv). In fact in this system the wettable silicon carbide 'substrate' is fabricated *in situ* and this process takes a certain time. The curves of figure 2 show first that the steady contact angles in the reactive and the non-reactive systems are nearly the same, and second that the contact angle decreases monotonically with time to its steady value, in disagreement with Aksay's model.

A slightly different procedure was used in another experiment performed with a Cu-1 at.% Cr alloy on a Cv substrate (Landry *et al.* 1997). Chromium promotes wetting of copper, forming at the interface a continuous layer a few microns in thickness of the wettable metallic-like chromium carbide Cr_7C_3. After cooling, the Cu–Cr solidified drop was dissolved, a small quantity of a Cu-1 at.% Cr alloy was placed in the centre of the carbide layer and the wetting experiment was repeated at the same temperature. Results (figure 3) are very similar to that of the Cu–Si alloy with respect to the following three points: (i) spreading in the reactive couple is much slower than in the corresponding non-reactive couple; (ii) the final contact angle formed by the Cu–Cr alloy on the initial substrate (C_v) and on the reaction product (chromium carbide) are nearly the same; and (iii) in the reactive system no minimum of θ is observed.

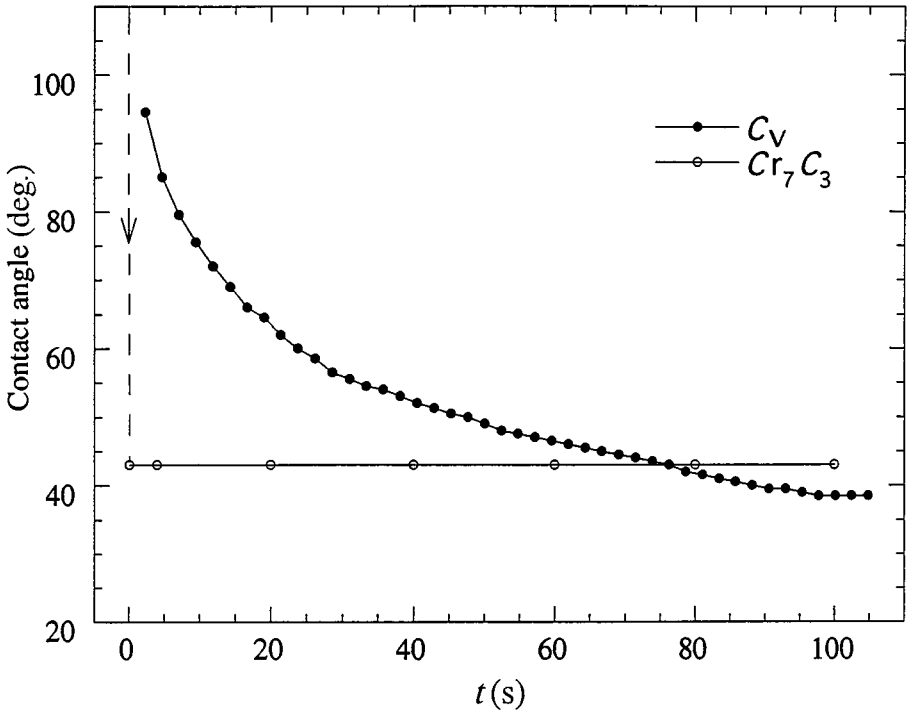

Figure 3. Contact angle versus time curves for a Cu-1 at.% Cr alloy on vitreous carbon and Cr_7C_3 substrates at 1373 K (Landry *et al.* 1997).

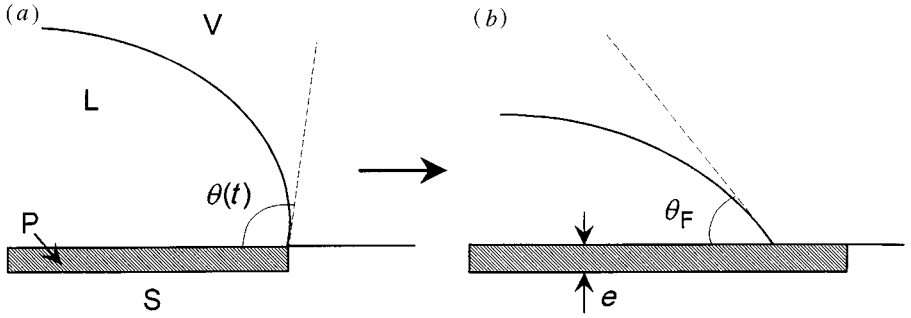

Figure 4. Instantaneous (a) and final (b) configuration at the solid–liquid–vapour triple line during spreading in reactive wetting.

From these and other experiments (Espié *et al.* 1994; Kritsalis *et al.* 1994), it was concluded that wetting in reactive systems correlates with the final interfacial chemistry at the triple line, not with the intensity of interfacial reactions (Eustathopoulos & Drevet 1993, 1994). Therefore, the reactive wetting driving force is

$$F_{\mathrm{d}}(t) = \sigma^0_{\mathrm{LV}}[\cos\theta_{\mathrm{F}} - \cos\theta(t)], \tag{2.4}$$

where θ_{F} is the equilibrium contact angle of the liquid on the reaction product surface (figure 4b) (note that this driving force is equal to the driving force in non-reactive-wetting of a liquid drop on an infinite surface of reaction product). The question discussed below is what are the processes which limit the velocity of the triple line when the contact angle changes from the initial contact angle to θ_{F}.

3. Spreading kinetics

In non-reactive systems, the spreading rate is controlled by the viscous flow and described (for $\theta < 60°$) by a power function of drop base radius R versus time t:

$$R^n \approx t, \tag{3.1}$$

in which n, as calculated by Tanner (1979) and by de Gennes (1985) is equal to 10.

Because the viscosity of molten metals is very low, the time needed for millimetre size droplets to reach capillary equilibrium is less than 10^{-1} s (Naidich 1981; Eremenko *et al.* 1994; Laurent 1988). This time is several orders of magnitude shorter than the spreading times observed in reactive metal-ceramic systems, usually lying in the range 10^1–10^4 s (Naidich 1981; Loehman & Tomsia 1988; Espié *et al.* 1994; Landry *et al.* 1997; Fujii *et al.* 1993; Nicholas & Peteves 1994; Mortimer & Nicholas 1970, 1973). Therefore in the latter systems the rate of spreading is not controlled by viscous resistance, but by the interfacial reaction itself. Another consequence of the low viscosity of the liquid is that during reactive spreading the drop radius is equal to the reaction product radius, i.e. the positions of the triple line and of the radial reaction front are identical.

Hereafter, spreading kinetics will be discussed by means of the classical two-step scheme used in treating kinetic phenomena, consisting of a local process at the interface and transport phenomena in bulk materials. The only difference in reactive wetting, but an important one, is that the relevant defect is not a two-dimensional interface but a line defect, the contact line of three phases S, L and V: because the liquid has a direct access to the solid at the triple line, the reaction rate at this particular point is two to three orders of magnitude higher than the reaction rate at the interface far from the triple line where the reaction occurs by slow diffusion through a solid layer (Landry & Eustathopoulos 1996).

In the framework of this general description, two limiting cases can be defined depending on the rate of the chemical reaction at the triple line compared to the rate of transport of reactive solute from the drop bulk to the triple line (or of a soluble reaction product from the triple line to the drop bulk).

(*a*) *Reaction-limited spreading*

In the first limit case chemical kinetics at the triple line are rate-limiting because transport within the droplet is comparatively rapid (or not needed when the drop is made of a pure reactive metal). In this case, (i) if the reaction does not change the global drop composition significantly, which means that the chemical environment of the triple line is constant with time and (ii) if a steady configuration is established at the triple line during wetting, then the rate of reaction and hence the triple line velocity are constant with time (Landry & Eustathopoulos 1996):

$$R - R_0 = Kt, \tag{3.2}$$

where R_0 is the initial drop base radius and K is a system constant, independent of the drop volume V_d.

An example is pure Al on vitreous carbon under high vacuum (figure 5) (Landry & Eustathopoulos 1996). In this system, wetting is promoted by the formation of a continuous layer of micron thickness of the wettable aluminium carbide at the interface, the final contact angle θ_F being about 70° (figure 5). After an initial stage, between time $t = 0$ and time $t_1 = 400$ s, due to deoxidation of the Al drop, the

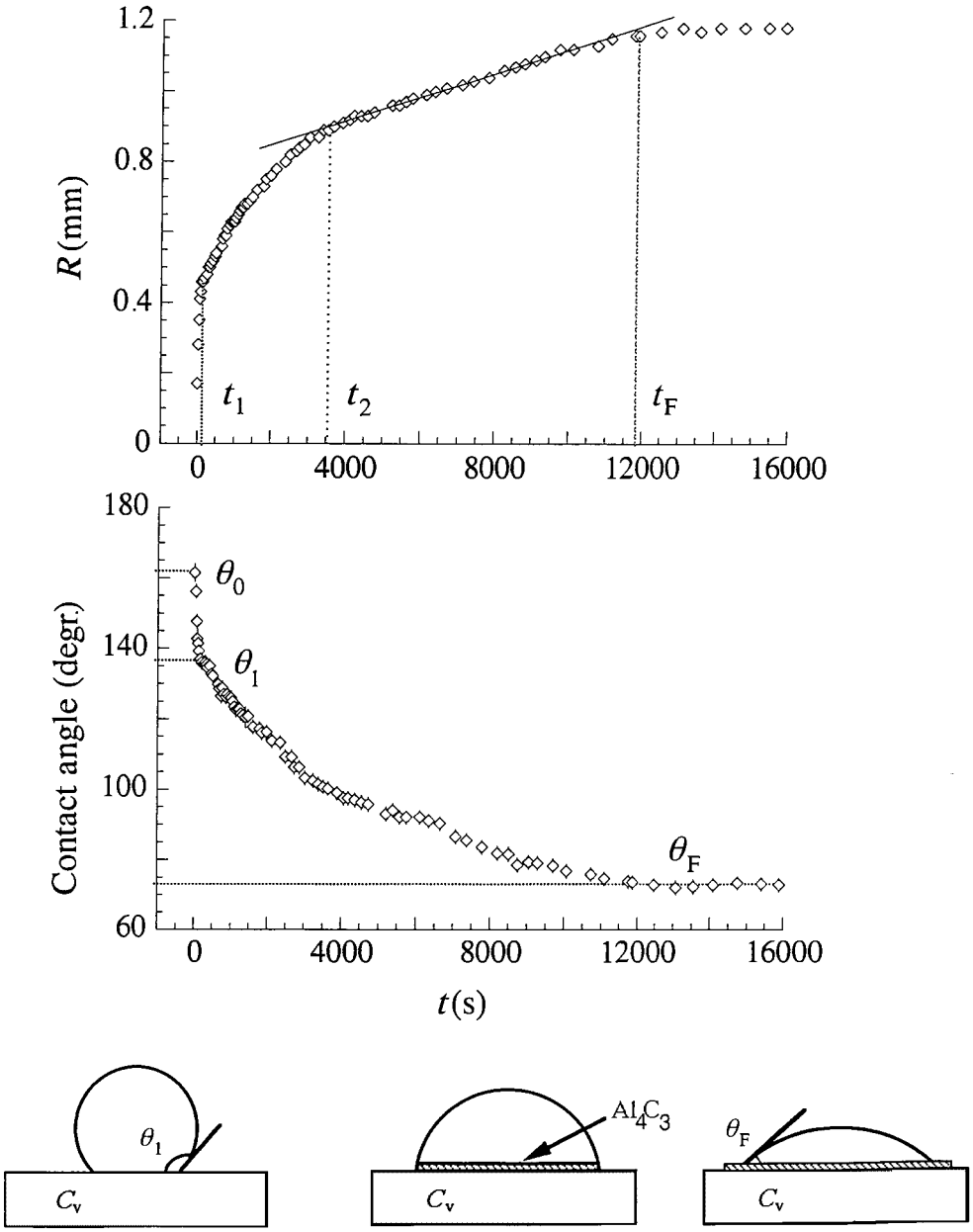

Figure 5. Variations with time of the contact angle and drop base radius observed in the Al/C_v system at 1100 K (Landry & Eustathopoulos 1996) and schematic representation of interfaces at $t = t_1$ (left), $t_2 < t < t_F$ (middle) and $t > t_F$ (right).

spreading curve $R(t)$ presents a nonlinear part (from t_1 to t_2) followed by a linear part (from t_2 to t_F).

The contact angle θ_1 is the contact angle of pure deoxidized Al on the original unreacted C_v surface (figure 5, bottom). θ_2 is the first contact angle corresponding to an interface fully covered by a reaction product layer. Therefore, the decrease from θ_1 to θ_2 corresponds to a transition from a non-reacted to a completely reacted

interface. For $t > t_2$, a steady configuration is established at the triple line and, as a result, the reaction rate and the triple line velocity are constant with time. During this stage the macroscopically observed contact angle is not related to capillary force equilibrium but is dictated by the drop volume and the radius of the reaction product layer. Indeed, the advance of the liquid is hindered by the presence of a non-wettable vitreous carbon in front of the triple line. Thus, the only way to move ahead is by lateral growth of the wettable carbide layer until the macroscopic contact angle equals the equilibrium contact angle of Al on the carbide.

This interpretation does not take into account the possible effect of a reaction occuring ahead of the triple line. In vacuum, such a reaction may occur by evaporation–condensation. For geometrical reasons (evidenced by considering the direction of evaporation with regard to the substrate surface) this mechanism is effective for non-wetting drops ($\theta > 90°$) and therefore may be, at least partially, responsible of the rapid spreading observed between t_1 and t_2 (figure 5) (Dezellus *et al.* 1998).

'Linear wetting' can occur in different systems and for different types of reaction. Examples are Cu–Si alloys on oxidized SiC (Rado 1997), the reactive Cu–Ag–Ti/Al_2O_3 system (Nicholas & Peteves 1995) or Cu–Si alloys on Cv (Landry *et al.* 1996; Dezellus *et al.* 1998). In some cases, small but significant deviations from linearity were observed and attributed to roughness of the reaction layer delaying the movement of the triple line by pinning (Landry & Eustathopoulos 1996).

(*b*) *Transport-limited spreading*

When local reaction rates are comparatively high, the rate of lateral growth of the reaction product at the triple line is limited by the supply of reactant from the drop bulk to the triple line. Because the contact angle decreases continuously during wetting, the reduction in transport field will lead to a continuous decrease in the reaction rate and, as a result, of the rate of movement of the triple line itself (figure 4). Therefore, time-dependent spreading rates are expected in this case (Landry & Eustathopoulos 1996).

In the liquid, solute is transported by convection and diffusion and the governing equation is Fick's second law written in the referential of the triple line moving with a velocity V_{TL} ($V_{\mathrm{TL}} = \mathrm{d}R/\mathrm{d}t$):

$$\frac{\partial C}{\partial t} + V_{\mathrm{F}} \cdot \nabla C = D\nabla^2 C + V_{\mathrm{TL}} \cdot \nabla C. \tag{3.3}$$

In this equation, the concentration C of reactive species is expressed in mass fraction. V_{F} denotes the local velocity of the fluid and results both from the movement of the triple line and from convection generated by temperature and concentration gradients in the liquid.

(i) *Pure diffusion*

Given the complexity of the real situation in the sessile drop configuration, a simplified analysis of diffusion-limited spreading has been proposed (Mortensen *et al.* 1997), in which it was assumed that in a small volume near the triple line diffusion is the dominating mechanism for solute transport. Inside this volume modelled as a straight wedge of angle θ (figure 6), the velocity V_{F} is taken equal to V_{TL} such that equation (3.3) reduces to

$$\frac{\partial C}{\partial t} = D\nabla^2 C. \tag{3.4}$$

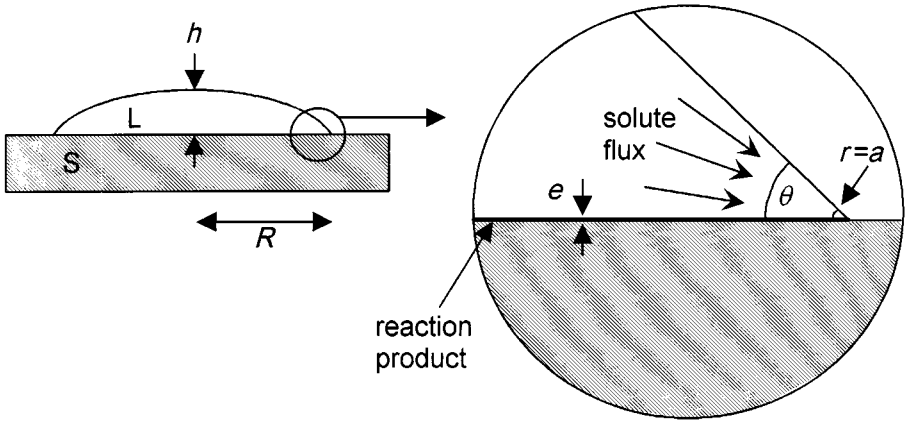

Figure 6. Schematic description of the advancing triple line driven by localized chemical reaction requiring solute transport in the liquid.

Neglecting the reaction at the interface far from the triple line, equation (3.4) was solved in cylindrical coordinates (r, Φ) (Mortensen *et al.* 1997). The main result of this analysis is that, although diffusion in the sessile drop configuration is basically unsteady, an accurate steady-state solution was found in which the reaction rate at the triple line, and hence the spreading rate, depends only on the configuration of the triple line or, in other words, on the instantaneous contact angle θ (Mortensen *et al.* 1997):

$$\frac{\mathrm{d}R}{\mathrm{d}t} = \frac{2DF(C_0 - C_\mathrm{e})\theta}{en_\mathrm{v}}. \tag{3.5}$$

In this equation, F is a constant close to 0.04, e is the thickness of the reaction product layer at the triple line and n_v is the number of moles of reactive species per unit volume of the reaction product. C_0 is the concentration of the reactive species in the bulk drop and C_e is the equilibrium concentration assumed to be attained inside a small volume of radius a near the triple line (see figure 6) (a being on the order of a few atomic jumps in the liquid, typically 10^{-9} m). Note that for the sake of homogeneity, the units of C_0 and C_e in equation (3.5) are moles per unit volume of the liquid. For millimetre-size droplets, forming nearly spherical cups, and contact angles not too high ($\theta \leqslant 60°$), θ is closely approximated by $4V_\mathrm{d}/\pi R^3$ where V_d is the drop volume. Equation (3.5) is then easily integrated to give

$$R^4 - R_0^4 = Kt, \tag{3.6}$$

where K is a constant for a given system, temperature, drop volume and concentration C_0.

In the framework of this model, solute gradients are localized near the triple line within a volume of radius δ approximately equal to $a\exp(1/(2F))$. For values of a of a few nm, δ is of the order of tens of micrometers. This discussion allows to check *a posteriori* the validity of the quasi-stationary approximation, using an approach similar to that followed in the related problem of mass transport ahead of a solidification interface (Garandet 1993). Indeed, let us denote τ the typical time scale of the composition field; the time-dependent and the Laplacian term in equation (3.4) will thus be proportional to $(1/\tau)$ and (D/δ^2), respectively. In our present problem, taking $\tau = 100$ s, $D = 3 \times 10^{-9}$ m^2 s^{-1} and $\delta = 20\,\mu$m, $D\tau/\delta^2$ is of the order of 1000 and the process can thus be safely taken as quasi-stationary.

Existing data on reactive wetting in metal–ceramic systems are usually given only as plots of contact angle versus time. Although from these results it may be concluded that in many systems spreading is nonlinear, no quantitative comparison between these data and equation (3.6) is possible. In a recent study, for the high reaction rate Cu-1 at.% Cr/C_v system, for which the spreading time is only 100 s, i.e. about 100 times shorter than in Al/C_v couple, the value of exponent n giving the best fit of the experimental $R(t)$ curves was found to be in the range 5.5–6.5 (Voitovich *et al.* 1998). These values are very different from $n = 10$, which is characteristic of viscous spreading, and from $n = 1$, typical of reaction-limited spreading. However, the values are higher than $n = 4$ calculated for pure diffusion. A possible reason for this disagreement is that convection in the drop has been neglected in this model.

(ii) *Convection*

In experimental practice, one can expect that solute will also be carried out by convective movements in the drop. Indeed, the density gradients related to temperature and composition differences interact with gravity to sustain a fluid motion. In addition, temperature and composition differences at the liquid–vapour interface give rise to Marangoni convection. To account for this convective effect, we shall rely on a former work carried out in a crystal growth configuration, where an equation similar to equation (3.3) governs solute repartition in the melt. It was seen in Garandet (1993) that both advection and convection could be combined in a single 'effective' velocity V_{eff}, defined as

$$V_{\mathrm{eff}} = D/\delta = V_{\mathrm{TL}} - V_{\mathrm{F}}(\delta), \tag{3.7}$$

where δ stands for the solutal boundary layer thickness. Note that with our choice of notation $V_{\mathrm{F}}(\delta)$, the fluid flow velocity at the boundary layer scale, is negative, but that V_{eff} is always positive (Garandet 1993).

In this section, we shall suppose that convection is a relevant mass transport mechanism, i.e. that fluid flow carries a significant amount of solute to the triple line. Whatever the physical origin of fluid flow, its expected effect will be to increase solute transport and to reduce the thickness δ of the solutal boundary layer in the vicinity of the triple line. In the mathematical formulation of the problem, we can thus safely neglect the time dependence of the composition field and consider the process as quasi-stationary, as discussed above. We thus look for a solution to the equation

$$D\nabla^2 C + V_{\mathrm{eff}} \cdot \nabla C = 0, \tag{3.8}$$

C being the solute composition expressed in mass fraction. At this point, V_{eff} should be taken as a mathematical auxiliary, but we shall return later to its physical basis.

In the frame of the present work, we are more interested in the identification of relevant transport mechanisms than with an accurate description of the problem geometry. We shall thus simplify matters and use a one-dimensional approach in Cartesian coordinates (see figure 7) to derive the composition gradient in the vicinity of the triple line. Equation (3.8) thus becomes

$$D\mathrm{d}^2C/\mathrm{d}x^2 + V_{\mathrm{eff}}\mathrm{d}C/\mathrm{d}x = 0. \tag{3.9}$$

The solution to equation (3.9), along with boundary conditions $C = C_{\mathrm{e}}$ in $x = a$ and $C = C_0$ as $x \to \infty$ is simply

$$C = \exp(V_{\mathrm{eff}}a/D)(C_{\mathrm{e}} - C_0)\exp(-V_{\mathrm{eff}}x/D) + C_0. \tag{3.10}$$

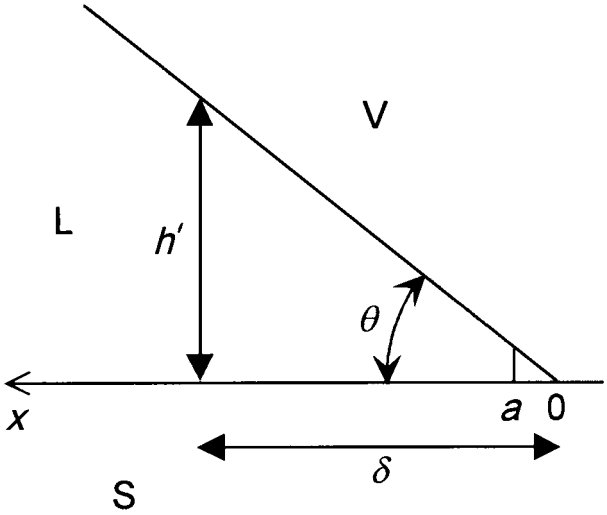

Figure 7. One-dimensional representation of the vicinity of the triple line at the solutal boundary layer scale δ.

Using this expression, the mass flux at the abscissa $x = a$ can be written as

$$|J| = \rho_{\mathrm{L}} D \left.\frac{\mathrm{d}C}{\mathrm{d}x}\right|_{x=a} = \rho_{\mathrm{L}}(C_0 - C_{\mathrm{e}})V_{\mathrm{eff}}, \tag{3.11}$$

where ρ_{L} is the mass density of the liquid. Assuming, that θ is small enough to ensure $\tan\theta \approx \theta$, the integrated mass flux at the abscissa $x = a$ is given by

$$|J_{\mathrm{t}}| = \rho_{\mathrm{L}}(C_0 - C_{\mathrm{e}})V_{\mathrm{eff}} 2\pi R\theta a. \tag{3.12}$$

In this expression of the total mass flux, we implicitly supposed convective transport to be negligible at the scale a, which is a fairly safe assumption. The mass balance in $x = a$ can be written as

$$\rho_{\mathrm{L}}(C_0 - C_{\mathrm{e}})V_{\mathrm{eff}}\theta a = \rho_{\mathrm{P}} C_{\mathrm{P}} e(\mathrm{d}R/\mathrm{d}t). \tag{3.13}$$

In the above expression ρ_{P} and C_{P} denote the mass density and the solute mass fraction of the product, respectively.

We now have to specify in more detail the physical sources of fluid flow in order to obtain quantitative informations about the spreading kinetics. Our first hypothesis will be to consider that solutal convection is negligible with respect to thermal convection. This may seem to be an *a priori* surprising assumption since it is well known that density and surface tension can both be very sensitive to the presence of solutes, even at low concentrations in the case of tensioactive species. However, we have seen that the composition variation, as evaluated by the pure diffusion model, occurs on a very limited length scale (*ca.* $\delta = 20\,\mu\mathrm{m}$), meaning that the flow has very little room to develop. Indeed, an order of magnitude analysis carried out in a recent work (Alboussiere *et al.* 1997) indicates that an *a priori* higher density gradient due to composition differences is less efficient as a convective driving force than temperature-induced density variations, the reason being that the latter take place over the whole fluid body. In the present paper, we shall only consider thermal convection but it should be kept in mind that in concentrated systems with large variations of density with composition, or in the case of tensioactive species, solutal convection could have an impact.

The next step is to estimate the relative influences of bulk and Marangoni convection in a spreading drop. To do so, we shall rely on the parallel flow solution obtained by Birikh (1966) in a layer of height h submitted to a constant thermal gradient, where the velocity at the liquid–vapour interface is given by

$$U = (\nu/h)[-\tfrac{1}{4}\, Re_{\mathrm{M}} + \tfrac{1}{48}\, Gr], \tag{3.14}$$

where ν represents the kinematic viscosity of the fluid. The non-dimensional Reynolds–Marangoni (Re_{M}) and Grashof (Gr) numbers are defined as

$$Re_{\mathrm{M}} = \sigma'_{\mathrm{T}} G h^2/\rho_{\mathrm{L}}\nu^2, \tag{3.15}$$

$$Gr = \beta_{\mathrm{T}} g G h^4/\nu^2. \tag{3.16}$$

The above expressions include thermophysical properties of the fluid, namely ρ_{L}, ν, σ'_{T}, derivative of its surface tension with respect to temperature and β_{T} its thermal expansion coefficient. The experimental conditions are characterized by h, the drop height, and G, the thermal gradient in the drop, with g denoting the acceleration due to gravity. Taking reasonable values, e.g. $\rho_{\mathrm{L}} = 10\,\mathrm{kg\,m^{-3}}$, $\nu = 3\times10^{-7}\,\mathrm{m^2\,s^{-1}}$, $\sigma'_{\mathrm{T}} = 2\times10^{-4}\,\mathrm{J\,m^{-2}\,K^{-1}}$, $\beta_{\mathrm{T}} = 10^{-4}\,\mathrm{K^{-1}}$, $g = 10\,\mathrm{m\,s^{-2}}$ and $h = 1\,\mathrm{mm}$, we get

$$Re_{\mathrm{M}} = 0.22G, \quad Gr = 0.01G \quad (G \text{ in } \mathrm{K\,m^{-1}}). \tag{3.17}$$

It thus appears clearly from equation (3.14) that bulk natural convection can be safely neglected in comparison with Marangoni convection. To quantify matters, we need to estimate the thermal gradient inside the drop. In typical sessile drop isothermal furnaces, residual thermal gradients lie between 0.1 and $0.5\,\mathrm{K\,mm^{-1}}$. Taking $Re_{\mathrm{M}} = 100$, we find that the fluid velocity in the drop is in the $\mathrm{cm\,s^{-1}}$ range. Incidentally, at such a limited value of Re_{M}, the flow is expected to be laminar.

Nevertheless, we still have to estimate the magnitude of the fluid velocity V_{F} at the composition boundary layer scale δ. As discussed in the related problem of solutal transport in crystal growth configurations (Garandet 1993), this is indeed the scale at which convection needs to be effective. Since we deal here with thin boundary layers, we should expect V_{F} to be significantly smaller than U. To get a rough estimate for $V_{\mathrm{F}}(\delta)$, we assume that the balance between surface tension and viscous forces used to derive equation (3.14) can be written at the boundary layer scale, i.e. when the drop height is h'. As can be seen in figure 7, h' and δ are related by $\tan\theta = h'/\delta$, meaning that they are of the same order of magnitude. The fluid velocity at the scale δ can thus be estimated as

$$V_{\mathrm{F}}(\delta) = (|\sigma'_{\mathrm{T}}|G/\rho_{\mathrm{L}}\nu)\tfrac{1}{4}h'. \tag{3.18}$$

Taking $h' = 40\,\mu\mathrm{m}$ (resp. $h' = 10\,\mu\mathrm{m}$) along with the above values and $G = 0.5\,\mathrm{K\,mm^{-1}}$ we get $V_{\mathrm{C}} = 300\,\mu\mathrm{m\,s^{-1}}$ (resp. $V_{\mathrm{C}} = 75\,\mu\mathrm{m\,s^{-1}}$). Assuming once more that θ is small enough to ensure $\tan\theta \approx \theta$, we get

$$V_{\mathrm{F}}(\delta) = (|\sigma'_{\mathrm{T}}|G/\rho_{\mathrm{L}}\nu)(\tfrac{1}{4}\delta\theta). \tag{3.19}$$

The above values of the convection velocity are indeed much smaller than U, but they are still significantly higher than the velocity of the triple line which is of the order of $10\,\mu\mathrm{m\,s^{-1}}$ in many practical cases (Voitovich *et al.* 1998; Drevet *et al.* 1996). We can thus assume that convection is indeed the dominant solute transport mode and drop the V_{TL} term in equation (3.7) or in other words set $V_{\mathrm{eff}} = -V_{\mathrm{F}}(\delta)$. The relation $V_{\mathrm{eff}} = D/\delta$ thus yields

$$\delta = 2(\rho_{\mathrm{L}}\nu D/|\sigma'_{\mathrm{T}}|G)^{1/2}\theta^{-1/2}. \tag{3.20}$$

Reporting this value of δ in equation (3.19) and in turn equation (3.19) in the mass balance equation (3.13), we get

$$(1/\theta^{3/2})\mathrm{d}R/\mathrm{d}t = \tfrac{1}{2}(\rho_\mathrm{L}/\rho_\mathrm{P})[(C_0 - C_\mathrm{e})/C_\mathrm{P}](a/e)(|\sigma'_\mathrm{T}|GD/\rho_\mathrm{L}\nu)^{1/2}. \tag{3.21}$$

Assuming once more that $\theta \ll 90°$ and setting $\theta = 4V_\mathrm{d}/\pi R^3$, we find that $R^{9/2}\,\mathrm{d}R/\mathrm{d}t$ is constant, and we finally get upon integration

$$R^{11/2} - R_0^{11/2} = \alpha t, \tag{3.22}$$

where α represents a proportionality factor given by

$$\alpha = 22/\pi^{3/2}(\rho_\mathrm{L}/\rho_\mathrm{P})[(C_0 - C_\mathrm{e})/C_\mathrm{P}](a/e)(|\sigma'_\mathrm{T}|GD/\rho_\mathrm{L}\nu)^{1/2}V_\mathrm{d}^{3/2}. \tag{3.23}$$

We have thus obtained an analytical expression for the drop spreading kinetics when temperature-driven Marangoni convection can be considered as the dominant solutal transport mechanism. Experimental results for the Cu-1 at.% $\mathrm{Cr/C_v}$ system (n = 5.5–6.5) (Voitovich *et al.* 1998) agree much better with equation (3.22) than with equation (3.6) established in the case of diffusive transport. Such a good agreement between experiment and the model based on Marangoni convection should be taken as coincidental in view of the large number of simplifying assumptions. The most significant result of this analysis is that in the case of millimetre-size droplets, Marangoni convection can significantly increase solutal transport with regard to the purely diffusive regime.

4. Conclusions

From the analysis of experimental data for model metal–ceramic systems, it appears that the final contact angle in a reactive system is given with good accuracy by Young's (or the equilibrium) contact angle of the liquid on the reaction product. Reactive systems feature either linear or nonlinear $R(t)$ spreading, corresponding to reaction-controlled and to transport-controlled regimes, respectively.

One of the purposes of the present study was to discuss the possible effects on spreading kinetics of various types of convection, i.e. thermal/solutal and bulk/Marangoni. Except for reactive solutes, which are also tensioactive at the liquid alloy free surface, or for alloys highly concentrated in reactive solutes, Marangoni convection generated by thermal gradients appears to be the most effective transport mode. Calculations show that, in the case of millimetre-size droplets, Marangoni convection can significantly modify the spreading law (exponent n and constant K in $R^n \approx Kt$) established for the purely diffusive regime. However, before concluding on the relative importance of the two transport mechanisms, i.e. convection and diffusion, current models have to be improved to take into account other phenomena likely to modify the values of n and K, namely some delocalization of the reaction ahead of the triple line (for instance by evaporation/condensation) or behind the triple line (by diffusion through the reaction product layer).

The authors acknowledge the significant contributions to different parts of this study made by Professor A. Mortensen (E. P. Lausanne), Dr R. Voitovich (from the Institute of Materials Science, Kiev), Dr K. Landry and Dr C. Rado (Grenoble). We thank Dr D. Camel (CEA-Grenoble) for fruitful discussions on the topic. The contribution of J. P. Garandet and B. Drevet was performed within the frame of the GRAMME agreement between the CNES and the CEA.

Appendix A. List of symbols

a	radius of the region where $C = C_e$
C	concentration of reactive species (mass fraction)
C_e	equilibrium concentration of reactive species (mass fraction)
C_0	concentration of reactive species in the bulk (mass fraction)
C_P	mass fraction of reactive species of the reaction product
D	diffusion coefficient in the liquid
e	thickness of the reaction product layer at the triple line
F	constant close to 0.04
F_d	wetting driving force
g	gravity acceleration
G	thermal gradient
Gr	Grashof number
h	height of the drop at its centre
h'	height of the drop at position δ
J	mass flux
J_t	total mass flux
K	constant of $R^n \approx Kt$ law
L	liquid
n	exponent of $R^n \approx Kt$ law
n_v	number of moles of reactive species per unit volume of the reaction product
P	reaction product
r	radius in cylindrical coordinates
R	drop base radius
R_0	initial drop base radius
Re_M	Reynolds Marangoni number
S	solid
Sc	Schmidt number
t	time
U	convective velocity at the L–V interface
V	vapour
V_d	drop volume
V_{eff}	effective velocity
V_F	velocity of the fluid
V_{TL}	velocity of the triple line
x	one-dimensional coordinate
β_T	thermal expansion coefficient
δ	thickness of the solute boundary layer
ΔG_r	change in Gibbs energy of the reaction
Φ	angle in cylindrical coordinates
ν	kinematic viscosity of the fluid
θ	contact angle
θ_F	final contact angle
ρ_L	mass density of the liquid
ρ_P	mass density of the reaction product
σ	surface energy
τ	time scale of reactive spreading
σ'_T	derivative of σ with respect to temperature

References

Aksay, I., Hoye, C. & Pask, J. 1974 *J. Phys. Chem.* **78**, 1178.

Alboussiere, T., Neubrand, A. C., Garandet, J. P. & Moreau, R. 1997 *J. Crystal Growth* **181**, 133.

Birikh, R. V. 1966 *J. Appl. Mech. Tech. Phys.* **3**, 43.

de Gennes, P. G. 1985 *Rev. Mod. Phys.* **57**, 289.

Dezellus, O., Hodaj, F. & Eustathopoulos, N. 1998 *Proc. 2nd Int. Conf. High Temperature Capillarity, Cracow, Poland, 1997* (ed. N. Eustathopoulos & N. Sobczac). (In the press.)

Drevet, B., Landry, K., Vikner, P. & Eustathopoulos, N. 1996 *Scripta Mater.* **35**, 1265.

Eremenko, V., Kostrova, L. & Lesnic, N. 1995 *Proc. Int. Conf. High Temperature Capillarity, Smolenice Castle, Slovakia, 1994* (ed. N. Eustathopoulos), p. 113.

Espié, L., Drevet, B. & Eustathopoulos, N. 1994 *Metall. Trans.* A **25**, 599.

Eustathopoulos, N. 1996 *Proc. 'Interface Science and Materials Interconnection' (JIMIS-8)*, pp. 61–68. The Japan Institute of Metals.

Eustathopoulos, N. & Drevet, B. 1993 *MRS Symp. Proc.* **314**, 15.

Eustathopoulos, N. & Drevet, B. 1994 *J. Physique* **4**, 1865.

Fujii, H., Nakae, H. & Okada, K. 1993 *Metall. Trans.* A **24**, 1391.

Garandet, J. P. 1993 *J. Crystal Growth* **131**, 431.

Kritsalis, P., Drevet, B., Valignat, N. & Eustathopoulos, N. 1994 *Scripta Metall. Mater.* **30**, 1127.

Landry, K. & Eustathopoulos, N. 1996 *Acta Metall. Mater.* **44**, 3923.

Landry, K., Rado, C. & Eustathopoulos, N. 1996 *Metall. Mater. Trans.* A **27**, 3181.

Landry, K., Rado, C., Voitovich, R. & Eustathopoulos, N. 1997 *Acta Metall. Mater.* **45**, 3079.

Laurent, V. 1988 Thesis, Institut National Polytechnique de Grenoble, France.

Loehman, R. & Tomsia, A. 1988 *Am. Ceram. Bull.* **67**, 375.

Mortensen, A., Drevet, B. & Eustathopoulos, N. 1997 *Scripta Mater.* **36**, 645.

Mortimer, D. & Nicholas, M. 1970 *J. Mater. Sci.* **5**, 149.

Mortimer, D. & Nicholas, M. 1973 *J. Mater. Sci.* **8**, 640.

Naidich, Y. 1981 *Progress in surface and membrane science* (ed. D. A. Cadenhead & J. F. Danielli), p. 353. New York: Academic.

Nicholas, M. 1986 *Br. Ceram. Trans. J.* **85**, 144.

Nicholas, M. & Peteves, S. 1995 *Proc. Int. Conf. High Temperature Capillarity, Smolenice Castle, Slovakia, 1994* (ed. N. Eustathopoulos), p. 18.

Nogi, K. 1993 *Trans. JWRI* **22**, 183.

Rado, C. 1997 Thesis, Institut National Polytechnique de Grenoble, France.

Tanner, L. 1979 *J. Phys.* D **12**, 1473.

Voitovich, R., Mortensen, A. & Eustathopoulos, N. 1998 *Proc. 2nd Int. Conf. High Temperature Capillarity, Cracow, Poland, 1997* (ed. N. Eustathopoulos & N. Sobczac). (In the press.)